Research in Diagnostic and Interventional Imaging 2 (2022) 100009

Contents lists available at ScienceDirect

Research in Diagnostic and Interventional Imaging

journal homepage: https://www.journals.elsevier.com/redii

Original article

Grading of soft tissues sarcomas using radiomics models: Choice of imaging methods and comparison with conventional visual analysis

Bailiang Chen[a,b,#], Olivier Steinberger[c,#], Roman Fenioux[a], Quentin Duverger[a], Tryphon Lambrou[d], Gauthier Dodin[c], Alain Blum[c], Pedro Augusto Gondim Teixeira[a,c,*]

[a] IADI, Inserm 1254 Nancy, University of Lorraine, Nancy, France
[b] Inserm CIC-IT 1433, University of Lorraine, Nancy, France
[c] Guilloz imaging department, Central Hospital, University Hospital Center of Nancy, 29 avenue du Maréchal de Lattre de Tassigny, Nancy cedex 54035, France
[d] School of Natural and Computing Sciences, University of Aberdeen, Meston Building, Old Aberdeen Campus, Meston Walk, Aberdeen AB24 3UE, United Kingdom

ARTICLE INFO

Article History:
Received 10 March 2022
Accepted 24 June 2022
Available online 2 July 2022

Keywords:
Tomography
X-Ray Computed
Magnetic resonance imaging
Radiomics
soft tissue sarcomas

ABSTRACT

Purpose: To determine which combination of imaging modalities/contrast, radiomics models, and how many features provides the best diagnostic performance for the differentiation between low- and high-grade soft tissue sarcomas (STS) using a radiomics approach.

Methods: MRI and CT from 39 patients with a histologically confirmed STS were prospectively analyzed. Images were evaluated both quantitatively by radiomics models and qualitatively by visual evaluation (used as reference) for grading (low-grade vs high-grade). In radiomics analysis, 120 radiomic features were extracted and contributed into three models: least absolute shrinkage and selection operator with logistic regression(LASSO-LR), recursive feature elimination and cross-validation (RFECV-SVC) and analysis of variance with SVC (ANOVA-SVC). Those were applied to different combinations of imaging modalities acquisition, with and without contrast medium administration, as well as selected number of features.

Results: Fat-saturated T2w (FS-T2w) MR images using RFECV-SVC radiomic models involving five features yielded the best results with mean sensitivity, specificity, and accuracy of 92% ± 10%, 78% ± 30%, and 89% ± 12%, respectively. The performance of radiomics was better than that of conventional analysis (67% accuracy) for STS grading. Combination of multiple contrast or imaging modalities did not increase the diagnostic performance.

Conclusion: FS-T2w MR images alone with a five-feature radiomics analysis usingh REFCV-SVC model may be able to provide sufficient diagnositic performance compared to conventional visual evaluation with multiple MRI contrast and CT imaging.

1. Introduction

Soft tissue sarcomas (STS) are a rare and heterogeneous group of lesions representing less than 1% of all tumors. The prognosis of patients with STS is dependent on tumor grade [1], which also strongly influences the therapeutic decision making [2]. Non invasive STS grading could have an impact on patient management as it could help prioritize and guide patients with more aggressive lesion to specialized cancer centers, with a potential prognostic benefit [3]. Improved non-invasive staging may potentially facilitate the management of STS reducing the need for percutaneous or surgical biopsy, thus could provide follow-up criteria for patients undergoing adjuvant therapy [4]. High-grade STS tend to present higher necrosis ratios and greater histological heterogeneity, which could be potentially assessed by texture analysis (TA). TA assesses the intensity heterogeneity of the pixels/voxels of an image through mathematical analysis, hence overcomes the limitation of subjective image interpretation [4-6]. Since the area under the receiver operator characteristics curve (AUC ROC) was often used to evaluate the diagnostic performance in terms of sensitivity and specificity, in TA, AUC ROC can be adopted as a metric to optimize the modelling procedure and

Abbreviations: LASSO, least absolute shrinkage and selection operator; LR, logistic regression; STS, soft tissue sarcoma; RFECV, recursive feature elimination and cross-validation; SVC, support vector classification; ROC AUC, receiver operator characteristics area under the curve; FNCLCC, French soft tumor grading system; VOI, volume-of-interest; IBSI, image biomarker standardization initiative; SMOTE, synthetic minority over-sampling technique; CE CT, contrast-enhanced CT; FS T1w, fat-saturated T1-weighted; CE FS T1w, Contrast-enhanced fat-saturated T1-weighted; FS T2w, fat-saturated T2-weighted

* Corresponding author.
E-mail address: ped_gt@hotmail.com (P.A. Gondim Teixeira).

# Olivier Steinberger and Bailiang CHEN have equal contribution to this manuscript and are co-first authors. Their positions on the author list follow the alphabetic order

https://doi.org/10.1016/j.redii.2022.100009

identify useful imaging features as potential endpoints imaging biomarkers [7].

In recent years, radiomics has been shown to improve lesion characterization by feeding a large number of features (e.g., texture parameters, geometry information, wavelet reconstruction, and histogram information) extracted from medical images to artificial intelligence based algorithms [6]. Radiomics improves lesion characterization and has shown a good correlation with histological tumor grades [5,8-10]. Although standardization of radiomics methods has been proposed, there is no consensus on the optimal imaging strategies (e.g., whether CT or MRI should be used, or whether contrast enhancement imaging is superior to native contrast, etc.) [11]. Moreover, the application of radiomics is technically complex and depends on various factors such radiomics algorithm, quantity, and quality of the texture features analyzed, all of which may have an impact on diagnostic performance. [10,12,13].

The reported performance of MRI-based radiomics for the differentiation between low- and high-grade STS varies in the literature (AUC ROC varying from 0.78 to 0.92) [10,12]. Additionally, CT based radiomics models have shown promise for the evaluation of tumors of various organs and systems (liver, bowel wall, lung, and kidney); however there is little information available on the application of this method for STS grading [14-19]. In this study, we sought to evaluate the diagnostic performance of radiomics for the differentiation between low- and high-grade STS with various imaging contrasts/modalities (fat-saturated T2-weighted, contrast enhanced fat-saturated T1-weighted MR image sequences, and contrast-enhanced CT) and technical factors (radiomics models and number of features).

2. Materials and methods

2.1. Patients selection

52 patients with a histologically confirmed STS who underwent contrast-enhanced MRI and contrast-enhanced CT from January 2010 to March 2017were initially identified in the clinical research Tumo-Osteo (Clinical trials number NCT02895633). All patients were adults and provided written informed consent. Seven patients without histological confirmation and one with important metallic artifacts were excluded. Five other patients were excluded because contrast-enhanced CT was not available. Thus, the final study population comprised 39 patients (Fig. 1). In this final population, there were 25 men and 14 women (M/F ratio = 1.8/), mean age 64 ± 16 (between 23 and 97). This retrospective study was approved by the local ethics committee.

2.2. Pathologic analysis

Tumor grade assessment was performed using needle core biopsy material for each tumor according to the French soft tumor grading system (FNCLCC [20]). FNCLCC grade I STS were considered as a group as these tumors can be considered as low-grade, and are often treated by surgery alone with a low risk of local or metastatic recurrence. FNCLCC grades II and III STS were grouped as these lesions can be considered as high-grade and usually require adjuvant chemotherapy and radiotherapy due to the risk of local recurrence and metastatic disease [21,22]. In the included population, there were eight grade I, 21 grade II, and 10 grade III STS, yielding eight low-grade and 31 high-grade tumors. The detailed histologic characteristics of the tumors studied are presented in Table 1.

2.3. Imaging acquisition

Each patient underwent MR and CT acquisitions on the same day. MR images were obtained from two different units: a 1.5T MR scanner (SignaHDxt 1.5T, GE Healthcare, Milwaukee, WI, USA) (34 patients), or a 3T MR scanner (Discovery MR750W 3.0 T, GE Healthcare, Milwaukee, WI, USA) (five patients). MR protocol included a fat- saturated using CHESS technique (FS), T2-weighted sequence, a non contrast enhanced (CE) FS T1-weighted sequence and a CE FS T1-weighted MR images sequence (contrast medium: 0.1 ml/Kg of Gadobenate Dimeglumine, Multihance® Bracco Imaging®, Milan, Italy). CT acquisitions (Aquilion One, Canon Medical Systems, Otawara, Japan) were performed the same day as MRI after contrast media injection (Iomeprol-400, Iomeron® Bracco Imaging®, Milan, Italy). Contrast medium (1.5-2ml/kg up to a maximum of 150ml) was injected at 4-5 ml/sec in a peripheral vein.

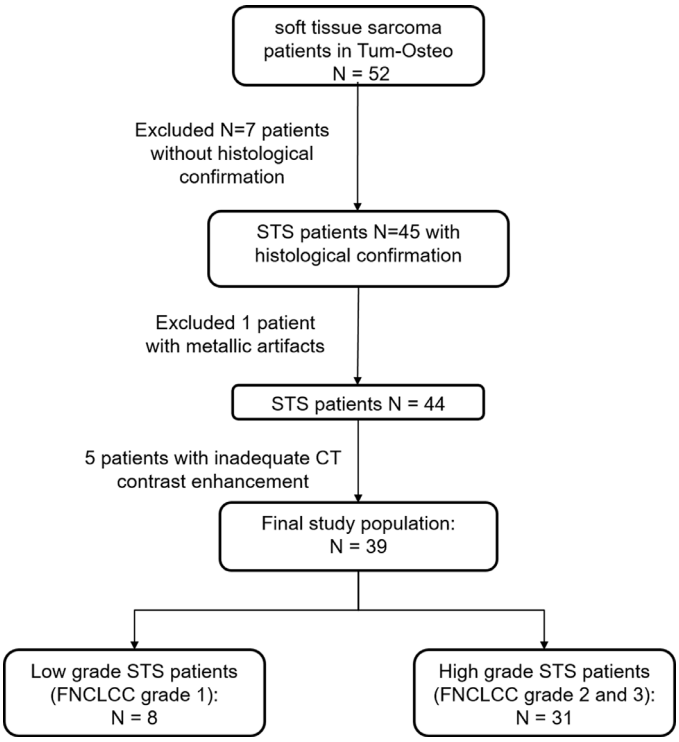

Fig. 1. Flow chart resuming the patients included and excluded with the final study population.

Table 1
Patient's demographic characteristics and histologic classification of the STS evaluated.

Characteristics	All patients	Low-Grade (Grade I)	High-Grade (Grade II and III)
Age (years)	64 ± 16	53 ± 19	67 ± 14
Gender			
Men	25 (64%)	6 (15%)	19 (49%)
Women	14 (36%)	8 (21%)	11 (28%)
Location			
Trunk*	6 (15%)	1 (3%)	5 (12%)
Extremities	33 (85%)	7 (18%)	26 (67%)
Final Grade			
I	8 (21%)		
II	21 (54%)		
III	10 (26%)		
Histological type			
Myxofibrosarcoma	7 (18%)	4 (10%)	3 (8%)
Leiomyosarcoma	2 (5%)	2 (5%)	
Myxoid liposarcoma	1 (3%)	1 (3%)	
Fusiform cell sarcorma	12 (31%)	1 (3%)	11 (28%)
Dermatofibrosarcoma protuberans	1 (3%)		1 (3%)
Rhabdomyosarcoma	2 (5%)		2 (5%)
Undifferentiated sarcoma	14 (36%)		14 (36%)

* three in the thoracic wall, one in the pelvis, one in the posterior cervical soft tissues, and one in the posterior abdominal wall

Table 2
MRI and CT acquisition parameters.

Modalities	MRI	CT	
Type of acquisition	T2w FS	CE T1w FS	CE CT
TR (ms)	2500-5277	665	
TE (ms)	44-75	11	
Flip angle (°)	80-90	90	
Bandwidth (kHz)	19-41.7	14.7-62.5	
NEX	2 - 6	1 - 3	
ETL*	8 - 22	2 - 4	
Gap (mm)*	0.2-3	0.2-3	
FOV (mm)*	156 × 100-521 × 300	140 × 90-521 × 300	200*160-
Matrix size*	224 × 224 −512 × 512	352 × 320-512 × 384	512 × 512
Slice thickness (mm)*	2 - 4	2 - 4	0.5**

* Parameter variation depending on patient body habitus.
** For CT, the slice thickness is "reconstruction slice thickness"
T2-weighted fat-saturated = T2w FS
Contrast-enhanced T1-weighted fat-saturated = CE T1w FS
Contrast-enhanced CT = CE CT
Field-of-view = FOV
Number of excitations = NEX
Echo train length = ETL

The acquisition parameters are detailed in Table 2 . Due to the various locations of STS, the resolution of MRI and CT varied from patient to patient.

2.4. Tumor segmentation

The MR data were segmented by a research radiographer (A.B.) by free hand tumor contouring on axial FS T2w and CE FS T1w sequences only using the ORS visual software (v.1985, Object Research Systems (ORS) Inc. Montreal, Quebec, Canada) and validated by a radiologist (O.S.) with three years of clinical experience in musculoskeletal radiology. CT images were segmented by the same radiologist (O.S.) with a software adapted to the segmentation of studies with a large number of slices using a "sparse segmentation" technique (e.g., the software does automatic contour interpolation based on the manual contouring of a few slices) (MITK 2016.11.10 v. Win64, Medical Imaging Interaction Toolkit, Heidelberg, Germany) (Fig. 2) [23]. The segmentation process was estimated to last 10 minutes per imaging modality.

2.5. Radiomics analysis

Image analysis was performed using the open source pyradiomics platfom with "Scikit-learn" library (v 3.7.5 Python software foundation, Beaverton, USA) following the image biomarker standardization initiative (IBSI) [17].

Preprocessing step: B-Spline interpolation was used to generate isotropic voxel size in all image data sets (pixel spacing and slice thickness were set to 0.4-0.6mm). Image datasets were also normalized to the scale of 0-100 and quantized within 20 bins to share a similar voxel intensity range. Voxels with intensity values outside the expected range were also removed.

Feature extraction step: In order to test what types of images are necessary when applying radiomics anlaysis in terms of providing better diagnostic performance, features were extracted using pyradiomics (IBSI proved, for detailed extracted feature types, see Fig. 3) in the following image set combinations:

- Set 1: Contrast-enhanced CT (CE CT);
- Set 2:T2-weighted fat-saturated (T2w FS);

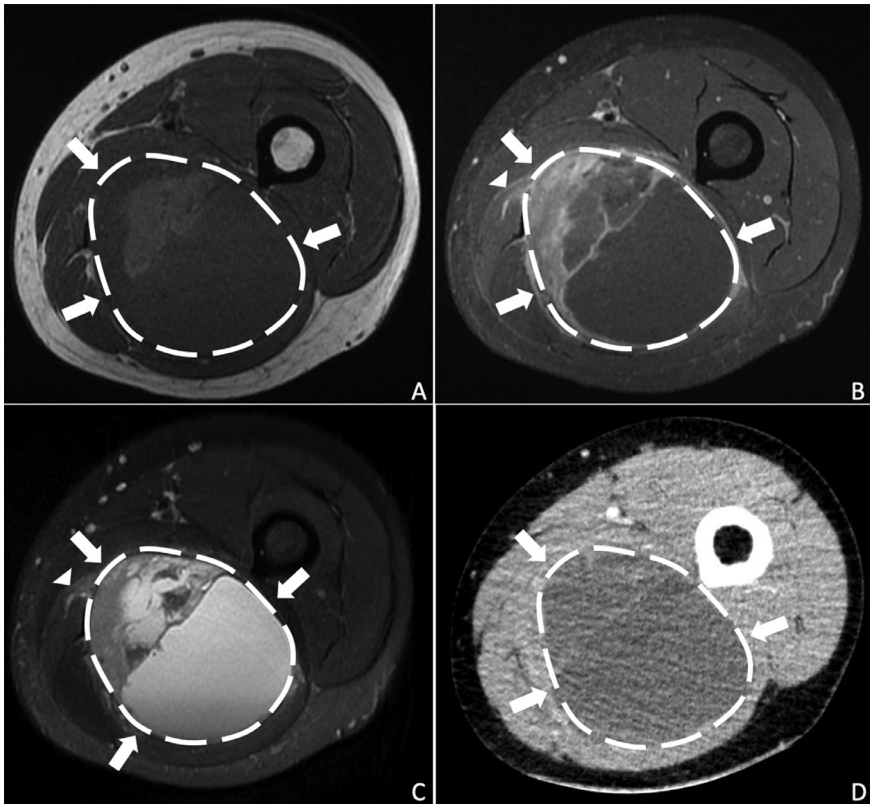

Fig. 2. Case of a 25-year-old male with a prior diagnosis of type I neurofibromatosis with a progressively enlarging mass of the posterior left thigh. Axial T1-weighted (A), axial fat-saturated contrast-enhanced T1-weighted (B), axial fat-saturated T2-weighted MR images (C) and axial contrast-enhanced CT (D) revealed a large mass in the posterior compartment of the left thigh. Pathological analysis was compatible with a malignant peripheral nerve sheath tumor of the sciatic nerve (white arrows). In each image, tumor boundaries are identified by a free-hand ROI (dashed white line).

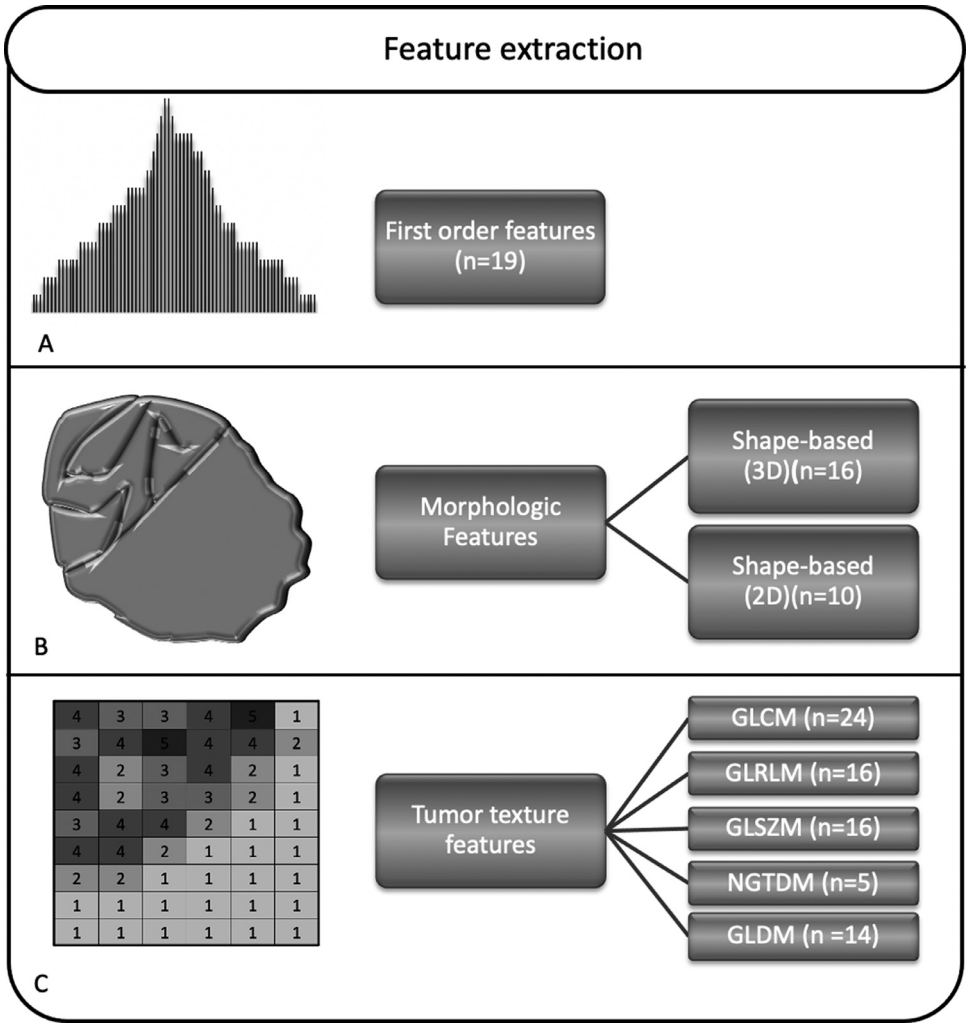

Fig. 3. Extracted feature types in pyradiomics. A) Histogram-based first-order features. B) Morphologic features related to the 2-D and 3-D tumor representation. C) Texture features derived from gray-level co-occurrence matrix (GLCM), gray level run length matrix (GLRLM), gray level size zone matrix (GLSZM), neighboring gray-tone difference matrix (NGTDM), and gray level dependence matrix (GLDM).

- Set 3: Contrast-enhanced T1-weighted fat-saturated (CE T1w FS);
- Set 4: both FS T2w and FS CE T1w FS (MR combined);
- Set 5: All images included (all combined)

Radiomics modelling step: After radiomics feature extraction, three commonly used radiomics models were applied, and each model included feature selection and grading:

- Recursive feature elimination with cross-validation (RFEVC) following a support vector classification (SVC) which eliminates the least important features making until the desired number of features is reached [24].
- Analysis of variance (ANOVA) which uses a univariate feature selection method also followed by a SVC technique.
- Logistic regression (LR) with least absolute shrinkage and selection operator (LASSO) technique used for feature selection [25].

Different number of selected features (five, 10, 15 and 20 features) were evaluated in all datasets and models.

75% of the evaluated datasets composed the training set, and the remaining 25% for the test set. Dataset selection was performed randomly using a stratified method that kept the same proportion of low- and high-grade tumors in either group. A nested cross-validation framework (50 iterations for the inner loop and 20 iterations for the outer loop) was implemented with the synthetic minority oversampling technique (SMOTE) to compensate for the problem of a small population with imbalanced groups. F1-score, accuracy and AUC ROC were output and used as metrics to optimize the radiomics models.

The computation time of each model per feature group was 3 mins for LASSO-LR, 1.9 mins for RFECV-SVC and 2.3 mins for ANOVA-SVC using a workstation, (CPU Intel Xeon W-2125, 32 G memory).

2.6. Visual tumor grading

Visual tumor grading was performed by a second radiologist (P.T.) with 11 years of clinical experience in musculoskeletal imaging, on MR sequences (FS T1w, FS T2w and CE FS T1w). The reader was blinded to histological findings. STS were classified as low or high grade considering various criteria reported in the literature: depth (superficial versus deep with respect to the superficial aponevrosis), size, tumor margin, intratumoral heterogeneous signal intensity on T2w images, and presence of non-enhancing tumor areas suggestive of necrosis [26-28].

2.7. Statistics

Statistical analysis was performed with Python software (v 3.7.5 Python software foundation, Beaverton, USA). Pathologic

analysis was considered as the standard of reference. The results for all models and all image datasets were exported to different confusion matrix to allow receiver operating characteristic (ROC) analysis. The sensitivity, specificity, accuracy, and the AUC ROC for the differentiation between low- and high-grade tumors were considered. The influence of the imaging modality, number of features, and radiomics model on diagnostic performance was evaluated considering all data available for each variable. One-way ANOVA was used to evaluate the statistical significance of differences in accuracy and ROC AUC in the subgroups studied. A p value of 0.05 was considered as the threshold of statistical significance. Quantitative data are presented as mean ± standard deviation (range).

3. Results

3.1. Radiomics models and number of features

The choice of radiomics model (i.e., RFECV-SVC, ANOVA-SVC, and LASSO-LR) significantly influenced the accuracy and ROC AUC values for the differentiation between low- and high-grade tumors (p = 0.001 and 0.01 for accuracy and ROC AUC, respectively). The RFECV-SVC model yielded the best performance with a mean accuracy and ROC AUC of 86% ± 4% and 89% ± 5%, respectively. The performance was slightly lower with ANOVA-SVC and LASSO-LR. A mean sensitivity and specificity of 90% ± 4% and 69% ± 12% could be reached with the RFECV-SVC model.

The number of features selected did not have a noticeable impact on the performance for STS tumor grading (p = 0.9). The mean accuracy and ROC AUC for the analysis of five, 10, 15, and 20 features varied from 81-82% ± 4-5% and 84-85% ± 6-7%.

3.2. Influence of imaging modalities

As the RFECV-SVC model presented the best performance for the differentiation of low- and high-grade STS, the evaluation of the performance of the different image modalities was performed with this model only using five features. The imaging modality significantly influenced accuracy and ROC AUC for the differentiation between low- and high-grade STS ($p < 0.0001$). FS T2w images alone presented the best overall performance with an accuracy and ROC AUC of 89% ± 12% and 94% ± 11%, respectively. The five following features from FS T2w MR images, shape flatness, GLSZM size zone nonuniformity, GLDM large dependence high gray level emphasis, GLCM informational measure of correlation 2, and 1st order minimum were identified (for detailed formula and definition of each features, please refer to [11]). The performance of CE CT only and of FS CE T1w only was slightly lower than that of FS T2w. Merging imaging modalities did not improve the overall performance for the differentiation between low- and high-grade STS. The best overall sensitivity (93% ± 7%) was reached when all image sets were merged, and the best overall specificity (85% ± 24%) was reached when the MR image sets were merged.

3.3. Visual evaluation

Regardless of the image set evaluated, radiomics analysis yielded better performance than visual tumor grading, which presented an accuracy of 67%. The sensitivity and specificity of the radiomics analysis of T2w FS images were also higher than that of visual tumor grading (Fig. 4).

The detailed results for all the analysis are presented in Table 3.

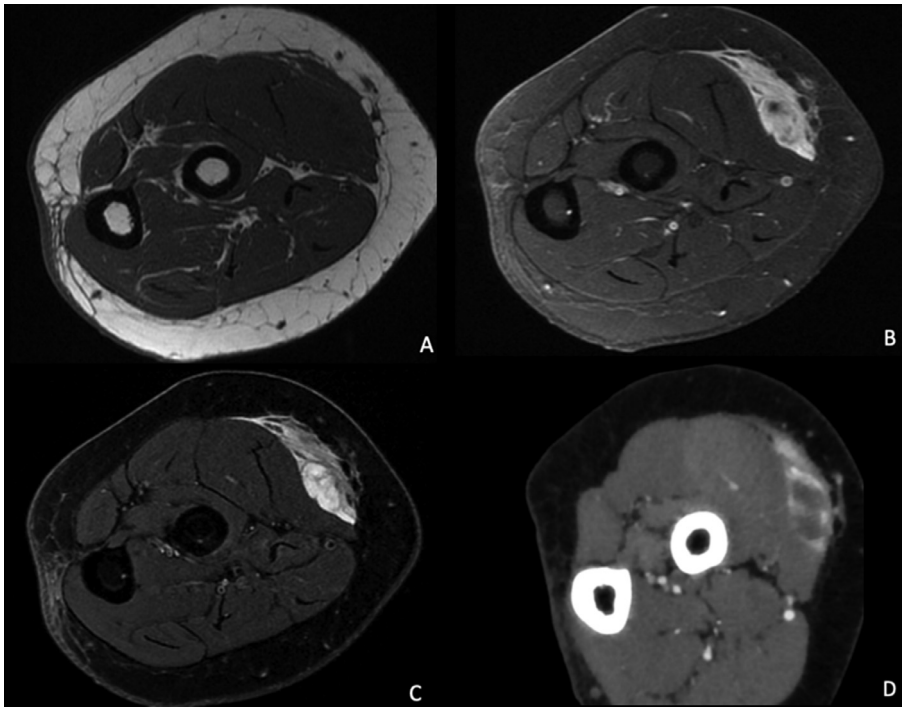

Fig. 4. Sixty-six years old women with a 3 month history of a left forearm subcutaneous antero lateral mass. Axial T1-weighted (A), axial contrast-enhanced T1-weighted fat-saturated (B), axial T2-weighted fat-saturated MR images (C), axial contrast-enhanced CT (D) showing a deep subcutaneous fusiform mass fusing along the the deep fascia of the forarm adjacent to the radiobrachialis muscle with irregular contours. On visual analysis, this tumor was classified as a low-grade with a single agressive criterium : irregular tumor margins. The texture analysis on T2-weighted fat-saturated with RFECV+SVC and 5 features classified this tumor in high grade and the final histologic diagnosis was that of a high grade tumor spindle cell sarcoma.

Table 3
Diagnostic performance of the radiomics for the differentiation between low- and high-grade STS. Best results in bold letters and in dark grey background.

Radiomics models	Nb of features	CE T1w FS				T2w FS				CE CT				MR combined†				ALL combined‡			
		Se	Spe	Acc	ROC	Se	Spe	Acc	ROC	Se	Spe	Acc	ROC	Se	Spe	Acc	ROC	Se	Spe	Acc	ROC
RFECV - SVC	5	86 ± 14	73 ± 34	83 ± 15	**89 ± 14**	**92 ± 10**	78 ± 30	**89 ± 12**	**94 ± 11**	**93 ± 9**	48 ± 20	84 ± 10	78 ± 20	86 ± 10	**85 ± 24**	86 ± 11	**94 ± 9**	**93 ± 7**	75 ± 26	**89 ± 9**	90 ± 13
	10	83 ± 10	58 ± 34	78 ± 11	82 ± 18	**92 ± 9**	**83 ± 24**	**90 ± 11**	**94 ± 10**	89 ± 9	53 ± 20	82 ± 10	85 ± 10	**90 ± 10**	73 ± 34	**87 ± 12**	**93 ± 9**	90 ± 10	**85 ± 24**	**89 ± 11**	**93 ± 9**
	15	83 ± 9	68 ± 34	80 ± 11	82 ± 15	**93 ± 9**	80 ± 25	**90 ± 10**	**95 ± 9**	**94 ± 8**	50 ± 23	85 ± 9	80 ± 22	**91 ± 8**	78 ± 30	**88 ± 11**	**92 ± 12**	**93 ± 7**	75 ± 26	**89 ± 9**	91 ± 12
	20	83 ± 11	**65 ± 29**	79 ± 11	81 ± 16	88 ± 12	75 ± 26	86 ± 11	91 ± 12	**95 ± 9**	48 ± 20	**86 ± 9**	83 ± 11	**93 ± 8**	75 ± 30	**90 ± 11**	**93 ± 12**	**92 ± 8**	65 ± 29	87 ± 10	91 ± 12
ANOVA - SVC	5	76 ± 8	63 ± 32	73 ± 9	78 ± 20	87 ± 9	73 ± 26	84 ± 10	86 ± 14	88 ± 13	53 ± 20	81 ± 13	77 ± 16	83 ± 9	73 ± 30	81 ± 9	90 ± 11	86 ± 13	60 ± 21	**81 ± 12**	87 ± 13
	10	79 ± 8	68 ± 34	77 ± 8	80 ± 18	81 ± 10	60 ± 26	77 ± 11	78 ± 18	88 ± 10	53 ± 20	81 ± 10	75 ± 14	87 ± 8	70 ± 30	84 ± 10	87 ± 15	**91 ± 9**	78 ± 26	88 ± 9	**92 ± 10**
	15	74 ± 9	63 ± 32	72 ± 12	73 ± 20	80 ± 13	63 ± 32	77 ± 13	84 ± 15	86 ± 11	60 ± 21	81 ± 11	77 ± 14	86 ± 8	**80 ± 25**	85 ± 9	90 ± 13	**94 ± 12**	60 ± 31	84 ± 13	88 ± 10
	20	75 ± 9	65 ± 33	73 ± 9	74 ± 18	85 ± 13	70 ± 25	82 ± 12	86 ± 12	85 ± 11	50 ± 16	78 ± 10	73 ± 15	86 ± 7	73 ± 30	84 ± 9	90 ± 12	90 ± 10	68 ± 29	86 ± 11	**92 ± 9**
LASSO -LR	5	81 ± 9	70 ± 30	79 ± 10	80 ± 14	86 ± 9	75 ± 26	84 ± 9	87 ± 13	82 ± 11	53 ± 20	76 ± 10	75 ± 14	85 ± 10	73 ± 30	83 ± 12	90 ± 11	86 ± 13	65 ± 24	82 ± 12	83 ± 15
	10	79 ± 8	68 ± 34	77 ± 10	**80 ± 16**	84 ± 8	70 ± 30	81 ± 10	86 ± 13	79 ± 11	55 ± 22	74 ± 9	72 ± 12	88 ± 8	73 ± 30	85 ± 10	88 ± 14	89 ± 8	**80 ± 25**	**88 ± 10**	**93 ± 9**
	15	77 ± 10	63 ± 32	74 ± 12	74 ± 17	84 ± 10	67 ± 37	81 ± 10	86 ± 17	81 ± 12	**65 ± 29**	78 ± 12	80 ± 12	88 ± 8	75 ± 26	86 ± 8	91 ± 12	89 ± 10	67 ± 29	85 ± 11	88 ± 11
	20	76 ± 6	65 ± 33	74 ± 9	77 ± 18	79 ± 15	67 ± 29	77 ± 14	85 ± 15	79 ± 10	58 ± 24	75 ± 11	75 ± 14	86 ± 8	73 ± 30	84 ± 10	89 ± 13	90 ± 10	67 ± 29	86 ± 11	91 ± 9

†MR combined: using both FS T2w and FS CE T1w data

‡All combined: using all the MR and CT data

4. Discussion

The radiomics (RFECV-SVC model on T2w FS images) yielded an overall performance for the differentiation between low- and high-grade STS (89% accuracy) and was better than that of visual evaluation of STS grading using the most commonly reported indicators of high-grade tumors (67% accuracy)(26–28). Compared to the literature, the radiomics performance was comparable to that reported by Zhang et al. [10] and superior to that reported by Peeken et al. [12], which could be related to the fact that a larger population was evaluated by the latter authors reducing the probability of an overtraining effect. This indicates a potential benefit of radiomics for non-invasive tumor grading, which might have implications in patient management.

The radiomics model and the imaging modality influenced the diagnostic performance of radiomics for the grading of STS ($p < 0.01$). The RFECV-SVC model yielded the best diagnostic performance for sarcoma grading in the study population. The radiomics model is a mathematical process that is influenced directly feature selection and sample classification, both paramount components of radiomics analysis. However, in the studied population the overall diagnostic performance was not influenced by the number of features evaluated. Using this model the best performance was obtained with FS T2w images, whereas the best sensitivity and specificity results were obtained using a combination of various imaging modalities. Although further confirmatory studies are necessary, the use of a single image modality (FS T2w images) with the RFECV-SVC model and any number of features can be proposed for non-invasive STS grading based on radiomics.

Contrary to what might be expected, radiomics based on CE FS T1w images yielded similar or worse results than the other image modalities evaluated. This could at least partially be explained by signal saturation effects in highly vascularized tumors artefactually reducing voxel heterogeneity. As CT is less sensitive to contrast saturation, this could also explain the differences in performance with respect to CE FS T1w images. The histological subtype could also have an distinct influence on the radiomics phenotype of each imaging modality, which could translate to differences in performance [12]. Although CE FS T1w MRI might not be the best option for a radiomics based tumor grading, contrast-enhanced MRI remains paramount for local staging and biopsy planning of soft tissue sarcoma [29].

There are several limitations to this work. Firstly, the number of STS evaluated was small and comprised tumors with various histologic subtypes. However, the main objective of this work was not to evaluate the diagnostic performance of radiomics in STS grading, but to evaluate the impact of the imaging protocol to radiomics models. Although the SMOTE technique was used to overcome this limitation [30], it has to be admitted that a bigger multi-centric study is necessary to generalize the conclusion in which other techniques such as balanced accuracy should be considered. Segmentation was not fully automatic and was time-consuming procedure, and can introduce subjective bias [31]. Other commonly used MRI sequences for the evaluation of soft-tissue tumors, such as T2 STIR, non contrast enhanced T1-weighted and post-contrast T1-weighted or T2-weighted sequences without fat saturation, were not evaluated in this study. The histological subtypes and the prognosis of pediatric soft tissue sarcoma is different than that of adults and were not evaluated in this study [32]. Pathological analysis was performed on core biopsy material instead of incisional biopsy which could have led to an underestimation of the tumor grade [33]. The influence of this issue was limited by the fact that tumors graded II and III were evaluated in association.

5. Conclusion

Radiomics analysis performed better than visual evaluation for the non-invasive grading of STS, confirming the potential role of this technique. The RFECV- SVC model applied to FS T2w images yielded the best overall performance to grade STS among the three imaging sets evaluated, even though the best sensitivity and specificity values were reached by merging these image sets. This information might have a positive impact on protocol optimization and post-processing for radiomics analysis of STS, potentially increasing the performance of non-invasive tumor grading.

Author contributions

Conceptualization: **Olivier Steinberger M.D, Bailiang Chen Ph.D., Alain Blum M.D, Ph.D., Pedro Augusto Gondim Teixeira M.D., Ph.D.**

Data curation: **Olivier Steinberger M.D., Bailiang Chen Ph.D., Quentin Duverger, Gauthier Dodin M.D., Alain Blum M.D, Ph.D., Pedro Augusto Gondim Teixeira M.D., Ph.D.**

Formal Analysis: **Olivier Steinberger M.D, Bailiang Chen Ph.D., Roman Fenioux, Quentin Duverger, Tryphon Lambrou Ph.D., Pedro Augusto Gondim Teixeira M.D., Ph.D.**

Funding acquisition: **NA**

Investigation: **Olivier Steinberger M.D., Bailiang Chen Ph.D., Alain Blum M.D, Ph.D., Pedro Augusto Gondim Teixeira M.D., Ph.D.**

Methodology: **Bailiang Chen Ph.D., Roman Fenioux, Quentin Duverger, Tryphon Lambrou Ph.D., Pedro Augusto Gondim Teixeira M.D., Ph.D.**

Project administration: **Pedro Augusto Gondim Teixeira M.D., Ph.D., Alain Blum M.D, Ph.D.**

Resources: **Bailiang Chen Ph.D., Pedro Augusto Gondim Teixeira M.D.**

Software: **Bailiang Chen Ph.D., Roman Fenioux, Quentin Duverger, Tryphon Lambrou Ph.D.,**

Supervision: **Bailiang Chen Ph.D., Pedro Augusto Gondim Teixeira M.D., Alain Blum M.D, Ph.D.**

Validation: **Bailiang Chen Ph.D., Pedro Augusto Gondim Teixeira M.D., Olivier Steinberger M.D., Tryphon Lambrou Ph.D., Quentin Duverger**

Visualization: **Bailiang Chen Ph.D., Olivier Steinberger M.D.,**

Writing – original draft: **Bailiang Chen Ph.D., Olivier Steinberger M.D., Pedro Augusto Gondim Teixeira M.D.,**

Writing – review & editing: **All the authors participated the reviewing and editing of the manuscript.**

Declaration of Competing Interest

Two authors of this manuscript (P.T. and A.B.) participated in a non-remunerated research agreement with Canon Medical Systems, manufacturer of the CT scanner used in this work.

The other authors of this manuscript declare no relationships with any companies whose products or services may be related to the subject matter of the article.

Acknowledgements

The authors would like to thank Ms, Agnes Basile for her help in segmentation and Mr. Yohann Mathieu-Daude for his help in feature analysis.

References

[1] Corey RM, Swett K, Ward WG. Epidemiology and survivorship of soft tissue sarcomas in adults: a national cancer database report. Cancer Med 2014;3(5):1404–15.

[2] Amin MB, Edge S, Greene F, Byrd DR, Brookland RK, Washington MK, editors. AJCC cancer staging manual. 8th edition Springer International Publishing: American Joint Commission on Cancer; 2017.

[3] Bonvalot S, Gaignard E, Stoeckle E, Meeus P, Decanter G, Carrere S, et al. Survival benefit of the surgical management of retroperitoneal sarcoma in a reference center: a nationwide study of the french sarcoma group from the NetSarc database. Ann Surg Oncol 2019;26(7):2286–93.
[4] Hayano K, Tian F, Kambadakone AR, Yoon SS, Duda DG, Ganeshan B, et al. Texture analysis of non-contrast enhanced CT for assessing angiogenesis and survival of soft tissue sarcoma. J Comput Assist Tomogr 2015;39(4):607–12.
[5] Dangoor A, Seddon B, Gerrand C, Grimer R, Whelan J, Judson I. UK guidelines for the management of soft tissue sarcomas. Clin Sarcoma Res 2016;6 [Internet] Available from: https://www.ncbi.nlm.nih.gov/pmc/articles/PMC5109663/.
[6] van Timmeren JE, Cester D, Tanadini-Lang S, Alkadhi H, Baessler B. Radiomics in medical imaging—"how-to" guide and critical reflection. Insights Imaging 2020;11(1):91.
[7] Feng XL, Wang SZ, Chen HH, Huang YX, Xin YK, Zhang T, et al. Optimizing the radiomics-machine-learning model based on non-contrast enhanced CT for the simplified risk categorization of thymic epithelial tumors: a large cohort retrospective study. Lung Cancer 2022;166:150–60.
[8] Tian F, Hayano K, Kambadakone AR, Sahani DV. Response assessment to neoadjuvant therapy in soft tissue sarcomas: using CT texture analysis in comparison to tumor size, density, and perfusion. Abdom Imaging 2015;40(6):1705–12.
[9] Peeken JC, Bernhofer M, Spraker MB, Pfeiffer D, Devecka M, Thamer A, et al. CT-based radiomic features predict tumor grading and have prognostic value in patients with soft tissue sarcomas treated with neoadjuvant radiation therapy. Radiother Oncol J Eur Soc Ther Radiol Oncol 2019.
[10] Zhang Y, Zhu Y, Shi X, Tao J, Cui J, Dai Y, et al. Soft tissue sarcomas: preoperative predictive histopathological grading based on radiomics of MRI. Acad Radiol 2019;26(9):1262–8.
[11] Zwanenburg A, Vallières M, Abdalah MA, Aerts HJWL, Andrearczyk V, Apte A, et al. The Image biomarker standardization initiative: standardized quantitative radiomics for high-throughput image-based phenotyping. Radiology 2020:191145.
[12] Peeken JC, Spraker MB, Knebel C, Dapper H, Pfeiffer D, Devecka M, et al. Tumor grading of soft tissue sarcomas using MRI-based radiomics. EBio Med 2019;48:332–40.
[13] Lambin P, Leijenaar RTH, Deist TM, Peerlings J, de Jong EEC, van Timmeren J, et al. Radiomics: the bridge between medical imaging and personalized medicine. Nat Rev Clin Oncol 2017;14(12):749–62.
[14] CT Texture Analysis: Definitions, Applications, Biologic Correlates, and Challenges. - PubMed - NCBI [Internet]. [cited 2019 Feb 5]. Available from: https://www.ncbi.nlm.nih.gov/pubmed/28898189
[15] Andersen MB, Harders SW, Ganeshan B, Thygesen J, Torp Madsen HH, Rasmussen F. CT texture analysis can help differentiate between malignant and benign lymph nodes in the mediastinum in patients suspected for lung cancer. Acta Radiol Stockh Swed 1987 2016;57(6):669–76.
[16] Suo S, Cheng J, Cao M, Lu Q, Yin Y, Xu J, et al. Assessment of heterogeneity difference between edge and core by using texture analysis: differentiation of malignant from inflammatory pulmonary nodules and masses. Acad Radiol 2016;23(9):1115–22.
[17] Hu Y, Liang Z, Song B, Han H, Pickhardt PJ, Zhu W, et al. Texture feature extraction and analysis for Polyp differentiation via computed tomography colonography. IEEE Trans Med Imaging 2016;35(6):1522–31.
[18] Raman SP, Schroeder JL, Huang P, Chen Y, Coquia SF, Kawamoto S, et al. Preliminary data using computed tomography texture analysis for the classification of hypervascular liver lesions: generation of a predictive model on the basis of quantitative spatial frequency measurements–a work in progress. J Comput Assist Tomogr 2015;39(3):383–95.
[19] Raman SP, Chen Y, Schroeder JL, Huang P, Fishman EK. CT texture analysis of renal masses: pilot study using random forest classification for prediction of pathology. Acad Radiol 2014;21(12):1587–96.
[20] Mandard AM, Petiot JF, Marnay J, Mandard JC, Chasle J, de Ranieri E, et al. Prognostic factors in soft tissue sarcomas. A multivariate analysis of 109 cases. Cancer 1989;63(7):1437–51.
[21] Casali PG, Abecassis N, Bauer S, Biagini R, Bielack S, Bonvalot S, et al. Soft tissue and visceral sarcomas: ESMO–EURACAN clinical practice guidelines for diagnosis, treatment and follow-up. Ann Oncol 2018;29:iv51–67.
[22] Toulmonde M, Le Cesne A, Mendiboure J, Blay JY, Piperno-Neumann S, Chevreau C, et al. Long-term recurrence of soft tissue sarcomas: prognostic factors and implications for prolonged follow-up. Cancer 2014;120(19):3003–6.
[23] Odille F, Bustin A, Liu S, Chen B, Vuissoz PA, Felblinger J, et al. Isotropic 3D cardiac cine MRI allows efficient sparse segmentation strategies based on 3D surface reconstruction. Magn Reson Med 2018;79(5):2665–75.
[24] Han J, Kamber M, Pei J. 9 - classification: advanced methods. In: Han J, Kamber M, Pei J, editors. Data mining. Third Edition Boston: Morgan Kaufmann; 2012. p. 393–442http://www.sciencedirect.com/science/article/pii/B9780123814791000095.
[25] Tibshirani R. Regression shrinkage and selection via the lasso: a retrospective. J R Stat Soc Ser B Stat Methodol 2011;73(3):273–82.
[26] Zhao F, Ahlawat S, Farahani SJ, Weber KL, Montgomery EA, Carrino JA, et al. Can MR imaging be used to predict tumor grade in soft-tissue sarcoma? Radiology 2014;272(1):192–201.
[27] Chhabra A, Ashikyan O, Slepicka C, Dettori N, Hwang H, Callan A, et al. Conventional MR and diffusion-weighted imaging of musculoskeletal soft tissue malignancy: correlation with histologic grading. Eur Radiol 2018.
[28] Liu QY, Li HG, Chen JY, Liang BL. Correlation of MRI features to histopathologic grade of soft tissue sarcoma. Ai Zheng Aizheng Chin J Cancer 2008;27(8):856–60.
[29] Noebauer-Huhmann IM, Weber MA, Lalam RK, Trattnig S, Bohndorf K, Vanhoenacker F, et al. Soft tissue tumors in adults: ESSR-approved guidelines for diagnostic imaging. Semin Musculoskelet Radiol 2015;19(5):475–82.
[30] Chawla NV, Bowyer KW, Hall LO, Kegelmeyer WP. SMOTE: synthetic minority over-sampling technique. J Artif Intell Res 2002;16:321–57.
[31] Xing S, Freeman C, Jung S, Levesque I. Automated segmentation of soft tissue sarcoma into distinct pathological regions using diffusion and T2 relaxation. In 2016.
[32] Ferrari A, Sultan I, Huang TT, Galindo CR, Shehadeh A, Meazza C, et al. Soft tissue sarcoma across the age spectrum: a population-based study from the surveillance epidemiology and end results database. Pediatr Blood Cancer 2011;57(6):943–9.
[33] Lin X, Davion S, Bertsch EC, Omar I, Nayar R, Laskin WB. Federation nationale des centers de lutte contre le cancer grading of soft tissue sarcomas on needle core biopsies using surrogate markers. Hum Pathol 2016;56:147–54.